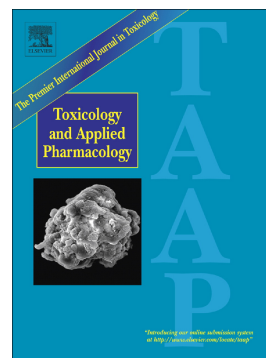


Journal Pre-proof

MiR-122-5p increases radiosensitivity and aggravates radiation-induced rectal injury through CCAR1

Yulong Ge, Wenzhi Tu, Junjun Li, Xuming Chen, Ying Chen, Yi Xu, Yiqing Xu, Yaming Wang, Yong Liu



PII: S0041-008X(20)30178-2

DOI: <https://doi.org/10.1016/j.taap.2020.115054>

Reference: YTAAP 115054

To appear in: *Toxicology and Applied Pharmacology*

Received date: 7 January 2020

Revised date: 26 April 2020

Accepted date: 12 May 2020

Please cite this article as: Y. Ge, W. Tu, J. Li, et al., MiR-122-5p increases radiosensitivity and aggravates radiation-induced rectal injury through CCAR1, *Toxicology and Applied Pharmacology* (2019), <https://doi.org/10.1016/j.taap.2020.115054>

This is a PDF file of an article that has undergone enhancements after acceptance, such as the addition of a cover page and metadata, and formatting for readability, but it is not yet the definitive version of record. This version will undergo additional copyediting, typesetting and review before it is published in its final form, but we are providing this version to give early visibility of the article. Please note that, during the production process, errors may be discovered which could affect the content, and all legal disclaimers that apply to the journal pertain.

© 2019 Published by Elsevier.

**MiR-122-5p increases radiosensitivity and aggravates
radiation-induced rectal injury through CCAR1**

Yulong Ge^{a,1}, Wenzhi Tu^{a,1}, Junjun Li^a, Xuming Chen^a, Ying Chen^a, Yi Xu^a, Yiqing Xu^a, Yaming Wang^{b*}, Yong Liu^{a*}

^aDepartment of Radiation Oncology, Shanghai General Hospital, Shanghai Jiao Tong University School of Medicine, Shanghai 201620, China

^bDepartment of General Surgery, HanDan Central Hospital, Handan 056001, China

¹These authors contributed equally to this work.

*Corresponding Authors:

Yong Liu, MD, PhD

Department of Radiation Oncology, Shanghai General Hospital, Shanghai Jiao Tong University School of Medicine, Shanghai 201620, China

Tel: 86-21-3779-8364

E-mail: yong.liu2@shgh.cn

Yaming Wang, MD

Department of General Surgery, HanDan Central Hospital, Handan 056001, China

Tel: 86-310-211-2584

E-mail: wymdz2008@163.com

Abstract

Radiation-induced rectal injury is a major side-effect observed in patients with pelvic malignancies who undergo radiotherapy. MicroRNA (miRNA), involved in many cellular biological processes, can be disturbed by ionizing radiation (IR). In this study, we have investigated the function of microRNA-122-5p (miR-122-5p) in radiation-induced rectal injury. MiR-122-5p levels in the serum of rectal cancer patients or in the rectal tissues of C57BL/6 mice before and after IR were detected by quantitative real-time PCR (qRT-PCR). We found that the miR-122-5p levels were significantly up-regulated in patients' serum or in mice rectal tissue after IR. Elevation of miR-122-5p levels sensitized human intestinal epithelial crypt (HIEC) cells to IR both *in vitro* and *in vivo*. MiR-122-5p mimic was transfected to HIEC cells and the downstream targets were predicted by bioinformatic analysis. Two putative target sites of miR-122-5p in the 3'UTR of the cell cycle and apoptosis regulator 1 (CCAR1) mRNA were found and verified by luciferase reporter assay. Overexpression of miR-122-5p or silencing CCAR1 combined with IR significantly inhibited cell survival, enhanced radiosensitivity, and increased cell apoptosis compared to that the negative control group *in vitro*. *In vivo* injection of miR-122-5p antagomir after IR significantly alleviated radiation-induced rectal injury in mice. These results suggest that miR-122-5p aggravates radiation-induced rectal injury through targeting CCAR1.

Keywords: miR-122-5p; CCAR1; Radiosensitivity; Rectal injury

1. Introduction

Radiotherapy is one of the important components of the comprehensive treatments for various pelvic malignancies. Radiotherapy not only kills the cancer cells, but also damages the adjacent normal tissues, resulting in various pelvic viscera injuries, including rectal injury. Radiation-induced rectal injury has many complications, of which radiation proctitis (RP) is a common one. RP is usually classified as acute radiation proctitis (ARP) and chronic radiation proctitis (CRP) (Do et al., 2011). ARP mostly occurs within 3 months after radiotherapy, mainly manifested as diarrhea, tenesmus, urgency, and rectal bleeding (Hong et al., 2001). CRP often occurs months to years after radiotherapy and is characterized by stricture, perforation, intestinal obstruction, and rectal bleeding (Do et al., 2011). About 10% of patients with pelvic malignancies who receive radiotherapy will develop CRP (Rustagi et al., 2015). Due to the difficulty in treatment, CRP seriously impairs patients' quality of life.

miRNAs are known as a class of small (20-24 nucleotides long), endogenous non-coding RNAs, which bind to the complementary sequences of target mRNAs, negatively regulating post-transcriptional target gene expression, resulting in translational repression or mRNA degradation. Many previous studies have indicated that miRNAs participate in various biological processes, including cell cycle regulation, proliferation, differentiation, and apoptosis (Mao et al., 2016; Zhou et al., 2018; Zheng et al., 2019). MiR-122-5p is located at chr18q21.31. Previous studies have revealed that miR-122-5p is abundantly found in hepatocytes and acts as a

biomarker of various hepatic diseases (Vliegenthart et al., 2017; Howell et al., 2018). Furthermore, recent studies have indicated that miR-122-5p is related to multiple organ damage. Wang et al. reported that miR-122-5p released from the injured liver cells caused pulmonary inflammation and tissue damage (Wang et al., 2019). Cisplatin-treated mice showed decreased miR-122-5p levels and developed acute kidney injury (Lee et al., 2014). Furthermore, overexpression of miR-122-5p promoted the apoptosis of H9C2 myocytes (Huang et al., 2012). Similarly, overexpression of miR-122-5p significantly induced H9C2 cell apoptosis in a hypoxia/reoxygenation rat model (Liang et al., 2016). It was further shown that the circulating miR-122-5p acted as an early biomarker for acute myocardial infarction (Cortez-Dias et al., 2016). In addition, miR-122-5p has been reported to improve radiosensitivity in A549 cells, leading to DNA double-strand breaks (DSBs) and cell apoptosis (Ma et al., 2015).

Taken together, miR-122-5p is an important miRNA involved in apoptosis in various types of cells. However, to date, there have been few reports of miR-122-5p associated with radiation-induced rectal injury. Therefore, in this study, we explored the function and the molecular mechanisms of miR-122-5p in radiation-induced rectal injury.

2. Materials and methods

2.1. Patient blood samples

Three patients diagnosed with rectal cancer were included in our study (from

HanDan Central Hospital), and patients' characteristics were detailed in Table 1. Blood samples were collected from patients before and after radiotherapy, and miRNA was extracted from serum immediately. The criteria from the 7th edition of the American Joint Committee of Cancer (AJCC) were utilized to classify various staging of tumors, lymph nodes, and metastasis (TNM). All patients received concurrent chemoradiotherapy (CCRT), and capecitabine 800 mg/m² orally, 6 days from the start of radiotherapy to the end of radiotherapy.

2.2. Cell line and Culture

The human intestinal epithelial crypt (HIEC) cell line, which was generously provided by the lab of Prof. Shao (Institute of Radiation Medicine, Fudan University, Shanghai, China), was cultured in RPMI-1640 medium (Gibco, Carlsbad, CA) supplemented with 10% fetal bovine serum (Gibco, Carlsbad, CA), 100 IU/mL of penicillin, and 100 mg/mL of streptomycin (Gibco, Carlsbad, CA) at 37°C with 5% CO₂ in an incubator.

2.3. Irradiation

The Oncor linear accelerator (Siemens, Amberg, Germany) was used to irradiate the HIEC cells and C57BL/6 mice with various doses at a dose rate of 3.5 Gy/min. The HIEC cells were irradiated with a single dose of 2 Gy, 4 Gy, 6 Gy, or 8 Gy. The abdomen of mice was exposed to a single dose of 25 Gy.

2.4. Animal studies

Female C57BL/6 mice (5-week-old, 20 g) were purchased from Shanghai Sippr-BK Laboratory Animal Co.Ltd. All mice were randomly divided into 4 groups and each group contained five mice: (i) non-IR group; (ii) 1 hour after 25 Gy IR group; (iii) 7 days after 25 Gy IR group; (iv) 14 days after 25 Gy IR group. At different time points after IR, mice were sacrificed by cervical dislocation and rectal tissues were collected for subsequent experiments.

2.5. Flow cytometry

The apoptotic cells were detected using Annexin V-FITC Apoptosis Detection Kit (BD Pharmingen TM, San Diego, CA). Briefly, HIEC cells were irradiated with 6 Gy after 48 hours of transfection with miR-122-5p mimic or CCAR1 small interfering RNA (siRNA). Forty-eight hours after IR, cells were resuspended in binding buffer, and stained with 5 μ L Annexin V-FITC and 5 μ L PI in the dark at room temperature for 15 minutes. Then, the apoptotic cells were analyzed with an Accuri C6 Flow cytometer (BD Biosciences, CA). The apoptosis rate was calculated as the early apoptosis rate plus the late apoptosis rate.

2.6. MicroRNA mimic or siRNA transfection

MiR-122-5p mimic, CCAR1 siRNA and negative controls were synthesized by Ribo Bio (Guangzhou, China). Twenty-four hours before transfection, HIEC cells were seeded into six-well plates, then transfected with 100 nM miR-122-5p mimic or

100 nM CCAR1 siRNA using Lipofectamine 2000 (Invitrogen, USA).

2.7. Plasmid transfection

The pcDNA3.1-FLAG-CCAR1 plasmid and pcDNA3.1 vector plasmid were synthesized by ViGene Biosciences (Shandong, China). Briefly, HIEC cells were seeded into six-well plates, then transfected with the plasmids using Lipofectamine 2000 (Invitrogen, USA).

2.8. Colony formation assay

HIEC cells transfected with miR-122-5p mimic or CCAR1 siRNA were seeded into six-well plates and divided into various dose IR (0 Gy, 2 Gy, 4 Gy, 6 Gy, and 8 Gy) groups, with different cells/well (100, 300, 600, 1000, and 2000 cells) added into each group, respectively. The cells were irradiated and cultured for 10-14 days. After incubation for 10-14 days, the culture medium was removed and the cell colonies were washed twice with cold PBS, fixed in methanol for 15 minutes, and then stained with 0.5% crystal violet staining solution for 15 minutes. The number of cells in colonies with more than 50 cells was counted. The single-hit multi-target model [$SF = 1 - (1 - e^{-D/D_0})^N$] in Graphpad Prism 7 software was used to plot survival curves and the survival fractions under different doses were calculated according to the curves.

2.9. Immunofluorescence microscopy

Forty-eight hours after IR, the transfected cells were harvested and fixed with

4% paraformaldehyde for 15 minutes, then permeabilized with 0.1% Triton X-100 for 15 minutes, and blocked with 1% BSA for 30 minutes at room temperature. Cells were then incubated with anti- γ -H2AX antibody (1:200, Cell Signaling Technology, Danvers, USA) overnight at 4°C. The next day, cells were incubated with Alexa Fluor 594 Goat Anti-Mouse IgG secondary antibody (1:200, Abcam, Cambridge, UK) for 1 hour in the dark. Nuclei were counterstained with 4', 6-diamidino-2-phenylindole (DAPI) (1:1000, Sigma, St. Louis, MO, USA). Images were acquired using Leica confocal microscope (Leica, Wetzlar, Germany).

2.10. RNA isolation and quantitative real-time PCR (qRT-PCR) analysis

miRNA was isolated from serum samples using the miRcute Serum/Plasma miRNA Isolation Kit (TianGen, Beijing, China). Total RNA was isolated from tissue or cell by using TRIzol reagent (Invitrogen, USA) according to the manufacturer's protocol. To quantify mRNA expression, PrimeScript RT Reagent Kit (Takara, Kyoto, Japan) was used to synthesize cDNA and the expression level was detected using SYBR Premix Ex Taq II (Takara, Kyoto, Japan). For miRNA quantification, cDNA was synthesized by miRcute Plus miRNA First-strand cDNA Kit (TianGen, Beijing, China) and the expression level was detected by miRcute Plus miRNA qPCR Detection Kit (TianGen, Beijing, China). Primers used in this study were listed in Table 2. GAPDH and U6 snRNA were used as endogenous controls. The $2^{-\Delta\Delta Ct}$ method was used to calculate the fold changes of miRNA or mRNA.

2.11. Luciferase reporter assay

For the luciferase reporter assay, 1×10^5 HEK293T cells/well were seeded into 24-well plates, then CCAR1-3'-UTR-wild-type and CCAR1-3'-UTR-mutant-type plasmids were co-transfected into HEK293T cells with miR-122-5p mimic or negative control using Lipofectamine 2000 (Invitrogen, USA). Forty-eight hours post transfection, luciferase activities were measured using Dual-Luciferase Reporter Assay Kit (Promega Corp., Madison, WI, USA) and renilla luciferase activities were used for normalization.

2.12. Mitochondrial membrane potential

To explore the effect of miR-122-5p or CCAR1 on the mitochondrial membrane potential, the JC-1 kit (Beyotime Biotech, Nantong, China) was selected for this experiment. HIEC cells transfected with miR-122-5p mimic or CCAR1 siRNA were irradiated with 6 Gy. Forty-eight hours post IR, the cells were washed with PBS twice, then resuspended in JC-1 solution, and incubated at 37°C for 30 minutes. The stained cells were measured using a confocal microscope (Leica, Wetzlar, Germany).

2.13. MicroRNA target prediction

Potential targets of miR-122-5p were predicted with three online software algorithms miRDB (<http://mirdb.org>), TargetScan (<http://www.targetscan.org>), and TargetMiner (https://www.isical.ac.in/~bioinfo_miu/targetminer20.htm). The common targets from the three databases were selected for further confirmation by luciferase

reporter assay and qRT-PCR.

2.14. Western blot analysis

The treated HIEC cells were washed with cold-PBS twice, and lysed in RIPA lysis buffer (Beyotime Biotech, Nantong, China) supplemented with protease and phosphatase inhibitors (Biomake, USA). The protein concentration was evaluated by BCA Protein Quantification kit (Thermo, USA). Then equal amount of protein (~20 µg) was separated by 10% SDS-PAGE gel and transferred to a PVDF membrane (Millipore, Billerica, MA). After 2 hours of blocking with 5% nonfat milk at room temperature, the membranes were incubated with the primary antibodies at 4°C overnight. Then the membranes were incubated with anti-rabbit (Cell Signaling Technology) or anti-mouse (Beyotime Biotech, Nantong, China) antibody for 1 hour at room temperature. The chemiluminescent detection system (P90719, Millipore Corporation, Billerica, MA, USA) was used to detect the signals from the PVDF membrane. The primary antibodies were as follows: CHK2 (1:1000, Cell Signaling Technology), phospho-CHK2 (Thr68) (1:1000, Cell Signaling Technology), GAPDH (1:1000, Cell Signaling Technology), and CCAR1 (1:1000, Absin, Shanghai, China).

2.15. Histopathology

Different time points (1 hour, 7 days, and 14 days) after 25 Gy IR or non-IR, the C57BL/6 mice were sacrificed. The rectal tissues were collected, fixed in 4% paraformaldehyde, and embedded in paraffin. Then, 3-µm-thick deparaffinized

sections were stained with H&E for further histopathological assessment.

2.16. Terminal deoxynucleotidyl transferase-mediated UTP nick-end labeling (TUNEL) assay

The degree of intestinal mucosal cell apoptosis was assessed using TUNEL apoptosis kit (In Situ Cell Death Detection Kit, AP, Roche). The TUNEL-positive cells were captured and analyzed using a microscope (Leica, Wetzlar, Germany).

2.17. Immunohistochemical (IHC) analysis

Immunohistochemistry experiments were performed on 3- μ m-thick deparaffinized sections of the tissue. In brief, the sections were incubated with anti-cl-caspase-3 (1:200, Cell Signaling Technology), phospho-CHK2 (Thr68) (1:200, Cell Signaling Technology), and CCAR1 (1:200, Absin, Shanghai, China) antibodies at 4°C overnight. Then the sections were incubated with secondary antibody for 30 minutes at room temperature. Three sections were selected randomly to count the apoptotic cells under a 200 \times microscope (Leica, Wetzlar, Germany).

2.18. miR-122-5p antagomir treatment

The abdomen of C57BL/6 mice was exposed to a single dose of 25 Gy IR. Immediately post IR, miR-122-5p antagomir or negative control (RiboBio, Guangzhou, China) 10 nM/48 hours (a total of 4 times) was injected by tail vein. Twenty-four hours after the last injection, mice were sacrificed and the rectal tissues

were collected for qRT-PCR, H&E, TUNEL staining, and IHC.

2.19. Statistical analysis

Graphpad Prism 7 software was used to analyze all the data. Statistical analysis between two groups was assessed by Student's *t*-test. All experiments were performed at least three times. Data were expressed as the mean \pm standard deviation. Differences were considered statistically significant when the p value was less than 0.05.

3. Results

3.1. Irradiation upregulates the miR-122-5p levels and promotes apoptosis in vivo

In order to investigate the relationship between IR and miR-122-5p, we first collected blood samples from three rectal cancer patients before and after radiotherapy. We found that the miR-122-5p levels in the serum of patients after radiotherapy were about 2 times higher than that before treatment (Fig. 1A). To prove the relationship between miR-122-5p and IR, we conducted further experiments with animal models. Therefore, we subjected the abdomen of C57BL/6 mice to irradiation with a single dose of 25 Gy IR or non-IR and collected rectal tissues at different time points after IR for qRT-PCR assay and histopathological examination. The qRT-PCR results showed that the miR-122-5p levels in the mice rectal tissues exposed to IR were significantly increased compared to non-IR group (Fig. 1B). H&E staining of rectal tissues showed obvious crypts shortening and atrophy in all IR groups compared to

the non-IR group (Fig. 1C). The results of TUNEL and cleaved caspase-3 showed that the number of apoptotic cells in all IR groups were higher than that in the non-IR group (Fig. 1C, 1D, and 1E). Altogether, these data indicate that irradiation upregulates the miR-122-5p expression and induces irreparable rectal injury.

3.2. Overexpression of miR-122-5p enhances the radiosensitivity of HIEC cells

To further explore the role of miR-122-5p in response to irradiation, HIEC cells were transfected with miR-122-5p mimic, and the transfection efficiency was confirmed by qRT-PCR (Fig. 2A). Next, we performed a colony formation assay to assess the role of miR-122-5p in radiosensitivity. As shown in Fig. 2B, we found that the survival fraction of HIEC cells transfected with miR-122-5p mimic was significantly decreased in 2 Gy, 4 Gy, 6 Gy, and 8 Gy IR compared to those transfected with miR-NC. In addition, to detect if the enhanced radiosensitivity was attributed to inducing DNA damage and activating apoptosis, we assessed the effects of miR-122-5p overexpression on DNA DSBs. We found that, with 6 Gy IR, γ -H2AX foci were significantly higher in miR-122-5p mimic transfected group than in the miR-NC group (Fig. 2C and 2D). Taken together, these results indicate that miR-122-5p overexpression enhances the formation of DNA DSBs.

We also performed a mitochondrial membrane potential assay to detect cell apoptosis. Decreased mitochondrial membrane potential ($\Delta\Psi_m$) is a sensitive event in the early stage of apoptosis and this change can be detected by the fluorescent probe JC-1. When $\Delta\Psi_m$ is high, JC-1 aggregates in the matrix of mitochondria, forming

polymers, and generating red fluorescence. Conversely, when $\Delta\Psi_m$ is low, JC-1 monomer generates green fluorescence, indicating early apoptosis. As shown in Fig. 2E, when compared to the miR-NC group, the HIEC cells transfected with miR-122-5p mimic showed strong green fluorescence upon treatment with 6 Gy IR. In addition, we performed a flow cytometry assay to examine the role of miR-122-5p in the apoptosis of HIEC cells exposed to 6 Gy IR (Fig. 2F). Results of apoptosis analysis showed that the apoptotic rate was significantly higher for the miR-122-5p overexpression+6 Gy IR group than that for the negative control group (Fig. 2G). These results suggest that miR-122-5p overexpression promotes irradiation-induced HIEC cells apoptosis.

3.3. *CCAR1* is a direct target of miR-122-5p

To explore the mechanism of miR-122-5p function in HIEC cells, we used 3 different online bioinformatic miRNA target prediction tools (miRDB, TargetScan, and TargetMiner) to search for the potential targets of miR-122-5p (Fig. 3A). A total of 19 targets were cross-linked in the three online software databases (Fig. 3B). Through literature search and biological function analyses, we chose 3 targets (*CCAR1*, *OCLN*, and *STK24*) for further confirmation. qRT-PCR results indicated that the relative mRNA expression of *CCAR1* significantly decreased while the expression of 2 other targets was upregulated when miR-122-5p mimic was transfected (Fig. 3C). These results indicated that *CCAR1* might be a direct target of miR-122-5p. Then, we adopted TargetScan database to predict the binding site

between miR-122-5p and CCAR1 (Fig. 3D). To validate our hypothesis, we performed the luciferase reporter assay and measured the luciferase activity. The relative luciferase activity was significantly suppressed when HEK293T cells were co-transfected with wild-type CCAR1 3'-UTR and miR-122-5p mimic compared to that observed in transfection with miR-NC. However, no obvious change in relative luciferase activity was found when the co-transfection of mutant-type CCAR1 3'-UTR with miR-122-5p mimic was performed in HIEC cells compared to that in the miR-NC group (Fig. 3E). In addition, western blot analysis confirmed that overexpression of miR-122-5p significantly decreased the CCAR1 protein levels (Fig. 3F). These results suggest that CCAR1 is a direct target of miR-122-5p.

3.4. Downregulation of CCAR1 enhances DNA radiosensitivity of HIEC cells

To explore the role of CCAR1 as a target of miR-122-5p in the IR-induced radiosensitivity of HIEC cells, two specific siRNAs against CCAR1 [RNA (i)-1, RNA (i)-2] were transfected into the HIEC cells and the transfection efficiency was evaluated by the levels of mRNA and protein (Fig. 4A and 4B). Next, a colony formation assay was performed to assess the role of CCAR1 in radiosensitivity. As shown in Fig. 4C and 4D, the survival fraction of HIEC cells transfected with CCAR1 siRNAs was significantly decreased in 2 Gy, 4 Gy, 6 Gy, and 8 Gy IR group compared to the si-NC group. These data showed that silencing CCAR1 could enhance the radiosensitivity of HIEC cells to IR. To explore the effects of CCAR1 on the DNA DSBs, immunofluorescence assay was performed to examine the γ -H2AX foci (Fig.

4E and 4F). As expected, IR increased the number of γ -H2AX foci as compared to that in the non-IR group, and the CCAR1 siRNA-transfected cells exposed to 6 Gy IR showed a significantly increased number of γ -H2AX foci as compared to the si-NC group (Fig. 4G and 4H). Next, we used fluorescent probe JC-1 to detect the apoptotic cells. As shown in Fig. 5A and 5B, strong green fluorescence was exhibited in the HIEC cells transfected with CCAR1 siRNAs combined with 6 Gy IR compared to the si-NC group. In addition, flow cytometry assay was conducted to examine whether CCAR1 was involved in cell apoptosis with or without IR (Fig. 5C and 5D). We found that, when the cells transfected with CCAR1 siRNAs were exposed to 6 Gy IR, the apoptosis rate were significantly increased compared to the si-NC treatment (Fig. 5E and 5F). These data suggest that downregulation of CCAR1 enhances radiosensitivity of HIEC cells exposed to IR.

3.5. miR-122-5p downregulated p-CHK2 levels through CCAR1 in HIEC cells after IR treatment

To further explore the mechanism of radiation-induced rectal injury, we treated HIEC cells with miR-122-5p mimic, CCAR1 siRNA or pcDNA3.1-FLAG-CCAR1 plasmid combined with 6 Gy IR or non-IR. The results of western blot showed that when HIEC cells transfected with miR-122-5p mimic or CCAR1 siRNA, the phosphorylation of check point kinase 2 (p-CHK2) was significantly increased after 6 Gy IR compared to that non-IR group (Fig. 6A and 6B). We also found that miR-122-5p overexpression or CCAR1 silencing combined with 6 Gy IR significantly

decreased the p-CHK2 expression compared to their negative controls (Fig. 6A and 6B). To further confirm CCAR1 was the direct target of miR-122-5p, we performed rescue experiment. We overexpressed CCAR1 on the basis of miR-122-5p transfection in HIEC cells. We found that miR-122-5p+CCAR1 overexpression combined with 6 Gy IR significantly increased the p-CHK2 expression compared to those transfected with miR-122-5p mimic group (Fig. 6C). Taken together, these data indicate that miR-122-5p may regulate radiosensitivity of HIEC cells by activating the CCAR1 signaling pathway, and CHK2 maybe participate in this process.

3.6. MiR-122-5p aggravates radiation-induced rectal injury *in vivo*

To investigate whether miR-122-5p could affect radiosensitivity *in vivo*, we established a model of radiation-induced rectal injury in C57BL/6 mice (Fig. 7A). Compared to the IR+NC group, the IR+miR-122-5p antagomir group showed significantly decreased miR-122-5p levels (Fig. 7B). Furthermore, we found that the levels of TUNEL and cleaved caspase-3 positive cells were higher in the IR + NC group than in the IR+miR-122-5p antagomir group (Fig. 7C, 7D, and 7E). In addition, in the IR+miR-122-5p antagomir group, the levels of CCAR1 and p-CHK2 were higher than those in the IR+NC group (Fig. 7C, 7F, and 7G). These data indicate that miR-122-5p inhibition decreases apoptosis and reduces IR-induced rectal injury via the CCAR1 signaling pathway *in vivo*. The schematic diagram of the molecular mechanism of miR-122-5p on radiation-induced rectal injury was also shown here (Fig. 8).

4. Discussion

Radiation-induced rectal injury is a major side-effect after radiotherapy in patients with pelvic malignancies, and its molecular mechanism remains unclear. On the one hand, many previous studies have shown that inflammation cytokine played an important role in RP. Bessout et al. found that T cells were activated and IL17 secreted by CD4 T cells enhanced inflammatory process and colonic mucosal regeneration in radiation-induced rectal injury after irradiation (Bessout et al., 2015). Symon et al. and Gerassy-Vainberg et al. found that IL-1 β and IL-6 levels were significantly increased in a mouse RP model (Symon et al., 2010; Gerassy-Vainberg et al., 2018). On the other hand, intestinal stem cells (ISCs) were also thought to participate in intestinal epithelial injury repair in response to IR. Tian et al. found that when ISCs were irradiated by high γ -IR, miR-31 levels were significantly increased, and then activated STAT3 signaling pathway to promote crypt regeneration in response to radiation-induced injury (Tian et al., 2017). A previous study also reported that unconventional prefoldin RPB5 interactor (URI) levels were significantly increased in the mouse intestinal crypt after high-dose irradiation and that overexpression of URI protected the mouse against radiation-induced gastrointestinal syndrome (GIS), while reduced URI expression sensitized the mouse intestinal epithelium to IR (Chaves-Perez et al., 2019). In addition, Blirando et al. showed that mast cells participated in RP and had deleterious effects (Blirando et al., 2011).

Previous studies have indicated that IR can alter miRNA expression. In our study,

we also found that miR-122-5p was up-regulated after IR and the injury of the mice rectal injury was most severe at 14 days after IR. Thus, we thought overexpression of miR-122-5p might be associated with radiation-induced rectal injury. MiR-122-5p is abundant in hepatocytes (Chang et al., 2004). It also exists in various types of cells and regulates apoptosis. For example, it has been indicated to promote apoptosis in endothelial cells (Li et al., 2019), in rat renal tubular epithelial cells (Qu and Zhang, 2018), and in H9C2 myocytes (Huang et al., 2012). In the current study, we also found that overexpression of miR-122-5p alone (non IR) induced HIEC cells apoptosis. These data show that miR-122-5p is pro-apoptotic. However, Lee and colleagues constructed a mouse model of acute kidney injury by treating mice with cisplatin; they found that miR-122-5p levels significantly decreased in the mice treated with cisplatin (Lee et al., 2014). Notably, miR-122-5p is also known to function as a tumor suppressor and promote cell apoptosis in many cancer cells (Ding et al., 2018; Liu et al., 2019). Previous studies have shown that cell sensitivity to radiation is associated with aberrant expression of miRNAs (Luo et al., 2019). In the present study, our results are consistent with many previous studies. For example, miR-122-5p enhanced radiosensitivity of A549 cells to IR. With 6 Gy ^{60}Co - γ IR, overexpression of miR-122-5p significantly enhanced the formation of γ -H2AX foci, and promoted cell apoptosis (Ma et al., 2015). The γ -H2AX foci are biomarkers of DNA DSBs (Lassmann et al., 2010). Ding et al. also derived the same conclusion; they found that overexpression of miR-122-5p significantly inhibited survival, enhanced radiosensitivity, and induced apoptosis in cervical cancer cells (Ding et al.,

2019). Similarly, from the results of the clonogenic survival assay, miR-122-5p was found to promote radiosensitivity and decrease survival in parental breast cancer cell lines, MCF-7 and MDA-MB-231. However, miR-122-5p was up-regulated in MCF-7RR and MDA-MB-231RR cells, and knockdown of miR-122-5p combined with radiation significantly promoted cell survival in both the radioresistant breast cancer cells line (Perez-Anorve et al., 2019). These data indicate that miR-122-5p has a dual function, dependent on the cell phenotype.

We found that CCAR1 was a direct target of miR-122-5p. Previously, Chang et al. reported that CCAR1 acted as a transcriptional coactivator of Wnt/ β -catenin signaling and reduction of CCAR1 by RNAi-mediated, suppressed cell growth, and induced apoptosis in gastric cancer cells (Chang et al., 2017). These results are consistent with our present study, where we showed that the reduction of CCAR1 alone (non-IR) inhibited HIEC cells growth and promoted apoptosis. Chen et al. also found a similar function of CCAR1 in lung cancer cells (Chen et al., 2018). They found that with different levels of glucose, splicing factor SRSF5 promoted CCAR1 to produce CCAR1L or CCAR1S proteins. Depletion of CCAR1S significantly suppressed cell growth, reduced colony-forming efficiency, and increased apoptosis. On the contrary, overexpression of CCAR1L notably reduced cell growth and colony formation, and increased apoptosis. CCAR1 also has dual functions in MCF-7 cells (Kim et al., 2008). On one hand, CCAR1 promoted cell proliferation by induction of estrogen; on the other hand, it enhanced apoptosis induced by DNA damage. Moreover, CCAR1 performs a pro-apoptotic role via diverse agents, including a

retinoid (CD437), chemotherapeutic adriamycin (doxorubicin), etoposide (Rishi et al., 2003), and epidermal growth factor receptor (EGFR) (Rishi et al., 2006). Taken together, these data may help to explain why CCAR1 performs diverse functions in different types of cells. However, the relationship between CCAR1 and IR is rarely reported. In our study, we found that the HIEC cells exposed to IR combined with CCAR1 siRNA significantly decreased survival, enhanced radiosensitivity, and induced cell apoptosis compared to the si-NC group.

CHK2 is an important regulator kinase activated in response to DNA damage response (Yuan et al., 2018). In the absence of DNA damage, CHK2 is not active. However, in response to IR-induced DNA damage, especially DSBs, CHK2 is mainly phosphorylated by the ataxia telangiectasia mutated (ATM) at Thr68 site (Hirao et al., 2000). CHK2 is a type of DNA damage repair protein (Abdel-Fatah et al., 2015; Angius et al., 2019). Liu et al. found that INK 128 combined with IR significantly decreased p-CHK2 and increased the radiosensitivity of MCF-7 cells (Liu et al., 2016). Wang et al. found that overexpression of c-MYC could lead to increase CHK1/2 expression, subsequently activated the DNA damage checkpoint response, and eventually resulted in radioresistance. However, decreased expression of CHK1/2 could overcome NPC radioresistance *in vitro* and *in vivo* (Wang et al., 2013). These data are consistent with our results that miR-122-5p overexpression or CCAR1 silencing combined with IR significantly decreased the p-CHK2 expression and enhanced radiosensitivity.

5. Conclusions

In this study, we demonstrated that overexpression of miR-122-5p can improve radiosensitivity of HIEC cells by targeting the CCAR1 and aggravated radiation-induced rectal injury. However, there are still some shortcomings in this study including few clinical samples. In the future, we will study the role of CHK2 regulated by miR-122-5p and CCAR1 in radiation-induced rectal injury, which may be good to know the radiation-induced rectal injury well.

Conflict of Interest

No conflicts of interest exist.

Acknowledgements

This work was supported by grants from the National Natural Science Foundation of China (Nos. 81872547, 81602663); the Natural Science Foundation of Shanghai (No.18ZR1430800); Scientific and Technological Innovation Action Plan of Shanghai Science and Technology Committee (No.19411950903) and Shanghai Municipal Education Commission-Gaofeng Clinical Medicine Grant Support (No. 20181713).

References

- Abdel-Fatah, T.M., Arora, A., Moseley, P.M., Perry, C., Rakha, E.A., Green, A.R., Chan, S.Y., Ellis, I.O., Madhusudan, S., 2015. DNA repair prognostic index

modelling reveals an essential role for base excision repair in influencing clinical outcomes in ER negative and triple negative breast cancers. *Oncotarget* 6, 21964-21978.

Angius, G., Tomao, S., Stati, V., Vici, P., Bianco, V., Tomao, F., 2019. Prexasertib, a checkpoint kinase inhibitor: from preclinical data to clinical development. *Cancer chemotherapy and pharmacology*.

Bessout, R., Demarquay, C., Moussa, L., Rene, A., Doix, S., Benderitter, M., Semont, A., Mathieu, N., 2015. TH17 predominant T-cell responses in radiation-induced bowel disease are modulated by treatment with adipose-derived mesenchymal stromal cells. *J Pathol* 237, 435-446.

Blirando, K., Milliat, F., Martelly, I., S. Bourin, J.C., Benderitter, M., Francois, A., 2011. Mast cells are an essential component of human radiation proctitis and contribute to experimental colorectal damage in mice. *Am J Pathol* 178, 640-651.

Chang, J., Nicolas, E., Marks, D., Sander, C., Lerro, A., Buendia, M.A., Xu, C., Mason, W.S., Moloshok, T., Bort, R., Zaret, K.S., Taylor, J.M., 2004. miR-122, a mammalian liver-specific microRNA, is processed from hcr mRNA and may downregulate the high affinity cationic amino acid transporter CAT-1. *RNA Biol* 1, 106-113.

Chang, T.S., Wei, K.L., Lu, C.K., Chen, Y.H., Cheng, Y.T., Tung, S.Y., Wu, C.S., Chiang, M.K., 2017. Inhibition of CCAR1, a Coactivator of beta-Catenin, Suppresses the Proliferation and Migration of Gastric Cancer Cells. *Int J Mol*

Sci 18.

Chaves-Perez, A., Yilmaz, M., Perna, C., de la Rosa, S., Djouder, N., 2019. URI is required to maintain intestinal architecture during ionizing radiation. *Science* 364.

Chen, Y., Huang, Q., Liu, W., Zhu, Q., Cui, C.P., Xu, L., Guo, X., Wang, P., Liu, J., Dong, G., Wei, W., Liu, C.H., Feng, Z., He, F., Zhang, L., 2018. Mutually exclusive acetylation and ubiquitylation of the splicing factor SRSF5 control tumor growth. *Nat Commun* 9, 2464.

Cortez-Dias, N., Costa, M.C., Carrilho-Ferreira, P., Silva, D., Jorge, C., Calisto, C., Pessoa, T., Robalo Martins, S., de Sousa, J.C., da Silva, P.C., Fiuza, M., Diogo, A.N., Pinto, F.J., Enguita, F.J., 2016. Circulating miR-122-5p/miR-133b Ratio Is a Specific Early Prognostic Biomarker in Acute Myocardial Infarction. *Circ J* 80, 2183-2191.

Ding, C.Q., Deng, W.S., Yin, X.F., Ding, X.D., 2018. MiR-122 inhibits cell proliferation and induces apoptosis by targeting runt-related transcription factors 2 in human glioma. *Eur Rev Med Pharmacol Sci* 22, 4925-4933.

Ding, F.N., Gao, B.H., Wu, X., Gong, C.W., Wang, W.Q., Zhang, S.M., 2019. miR-122-5p modulates the radiosensitivity of cervical cancer cells by regulating cell division cycle 25A (CDC25A). *FEBS open bio* 9, 1869-1879.

Do, N.L., Nagle, D., Poylin, V.Y., 2011. Radiation proctitis: current strategies in management. *Gastroenterol Res Pract* 2011, 917941.

Gerassy-Vainberg, S., Blatt, A., Danin-Poleg, Y., Gershovich, K., Sabo, E., Nevelsky,

- A., Daniel, S., Dahan, A., Ziv, O., Dheer, R., Abreu, M.T., Koren, O., Kashi, Y., Chowers, Y., 2018. Radiation induces proinflammatory dysbiosis: transmission of inflammatory susceptibility by host cytokine induction. *Gut* 67, 97-107.
- Hirao, A., Kong, Y.Y., Matsuoka, S., Wakeham, A., Ruland, J., Yoshida, H., Liu, D., Elledge, S.J., Mak, T.W., 2000. DNA damage-induced activation of p53 by the checkpoint kinase Chk2. *Science* 287, 1824-1827.
- Hong, J.J., Park, W., Ehrenpreis, E.D., 2001. Review article: current therapeutic options for radiation proctopathy. *Aliment Pharmacol Ther* 15, 1253-1262.
- Howell, L.S., Ireland, L., Park, B.K., Gearing, C.E., 2018. MiR-122 and other microRNAs as potential circulating biomarkers of drug-induced liver injury. *Expert Rev Mol Diagn* 18, 47-54.
- Huang, X., Huang, F., Yang, D., Cong, F., Shi, X., Wang, H., Zhou, X., Wang, S., Dai, S., 2012. Expression of microRNA-122 contributes to apoptosis in H9C2 myocytes. *J Cell Mol Med* 16, 2637-2646.
- Kim, J.H., Yang, C.K., Heo, K., Roeder, R.G., An, W., Stallcup, M.R., 2008. CCAR1, a key regulator of mediator complex recruitment to nuclear receptor transcription complexes. *Mol Cell* 31, 510-519.
- Lassmann, M., Hanscheid, H., Gassen, D., Biko, J., Meineke, V., Reiners, C., Scherthan, H., 2010. In vivo formation of gamma-H2AX and 53BP1 DNA repair foci in blood cells after radioiodine therapy of differentiated thyroid cancer. *Journal of nuclear medicine : official publication, Society of Nuclear*

Medicine 51, 1318-1325.

Lee, C.G., Kim, J.G., Kim, H.J., Kwon, H.K., Cho, I.J., Choi, D.W., Lee, W.H., Kim, W.D., Hwang, S.J., Choi, S., Kim, S.G., 2014. Discovery of an integrative network of microRNAs and transcriptomics changes for acute kidney injury. *Kidney Int* 86, 943-953.

Li, Y., Yang, N., Dong, B., Yang, J., Kou, L., Qin, Q., 2019. MicroRNA-122 promotes endothelial cell apoptosis by targeting XIAP: Therapeutic implication for atherosclerosis. *Life Sci* 232, 116590.

Liang, W., Guo, J., Li, J., Bai, C., Dong, Y., 2015. Downregulation of miR-122 attenuates hypoxia/reoxygenation (H₂O₂)-induced myocardial cell apoptosis by upregulating GATA-4. *Biochemical Biophys Res Commun* 478, 1416-1422.

Liu, Y.H., Liu, J.L., Wang, Z., Zhu, X.H., Chen, X.B., Wang, M.Q., 2019. MiR-122-5p suppresses cell proliferation, migration and invasion by targeting SATB1 in nasopharyngeal carcinoma. *Eur Rev Med Pharmacol Sci* 23, 622-629.

Liu, Z.G., Tang, J., Chen, Z., Zhang, H., Wang, H., Yang, J., Zhang, H., 2016. The novel mTORC1/2 dual inhibitor INK128 enhances radiosensitivity of breast cancer cell line MCF-7. *Int J Oncol* 49, 1039-1045.

Luo, A., Zhou, X., Shi, X., Zhao, Y., Men, Y., Chang, X., Chen, H., Ding, F., Li, Y., Su, D., Xiao, Z., Hui, Z., Liu, Z., 2019. Exosome-derived miR-339-5p mediates radiosensitivity by targeting Cdc25A in locally advanced esophageal squamous cell carcinoma. *Oncogene* 38, 4990-5006.

- Ma, D., Jia, H., Qin, M., Dai, W., Wang, T., Liang, E., Dong, G., Wang, Z., Zhang, Z., Feng, F., 2015. MiR-122 Induces Radiosensitization in Non-Small Cell Lung Cancer Cell Line. *Int J Mol Sci* 16, 22137-22150.
- Mao, A., Zhao, Q., Zhou, X., Sun, C., Si, J., Zhou, R., Gan, L., Zhang, H., 2016. MicroRNA-449a enhances radiosensitivity by downregulation of c-Myc in prostate cancer cells. *Sci Rep* 6, 27346.
- Perez-Anorve, I.X., Gonzalez-De la Rosa, C.H., Soto-Reyes, E., Beltran-Anaya, F.O., Del Moral-Hernandez, O., Salgado-Albarra, M., Angeles-Zaragoza, O., Gonzalez-Barrios, J.A., Landero-Huerta, D.A., Chavez-Saldana, M., Garcia-Carranca, A., Villegas-Sepulveda, N., Arechaga-Ocampo, E., 2019. New insights into radioresistance in breast cancer identify a dual function of miR-122 as a tumor suppressor and oncomiR. *Mol Oncol* 13, 1249-1267.
- Qu, X.H., Zhang, K., 2018. MiR-122 regulates cell apoptosis and ROS by targeting DJ-1 in renal ischemic reperfusion injury rat models. *Eur Rev Med Pharmacol Sci* 22, 8830-8838.
- Rishi, A.K., Zhang, L., Boyanapalli, M., Wali, A., Mohammad, R.M., Yu, Y., Fontana, J.A., Hatfield, J.S., Dawson, M.I., Majumdar, A.P., Reichert, U., 2003. Identification and characterization of a cell cycle and apoptosis regulatory protein-1 as a novel mediator of apoptosis signaling by retinoid CD437. *J Biol Chem* 278, 33422-33435.
- Rishi, A.K., Zhang, L., Yu, Y., Jiang, Y., Nautiyal, J., Wali, A., Fontana, J.A., Levi, E., Majumdar, A.P., 2006. Cell cycle- and apoptosis-regulatory protein-1 is

- involved in apoptosis signaling by epidermal growth factor receptor. *J Biol Chem* 281, 13188-13198.
- Rustagi, T., Corbett, F.S., Mashimo, H., 2015. Treatment of chronic radiation proctopathy with radiofrequency ablation (with video). *Gastrointest Endosc* 81, 428-436.
- Symon, Z., Goldshmidt, Y., Picard, O., Yavzori, M., Ben-Horin, S., Alezra, D., Barshack, I., Chowers, Y., 2010. A murine model for the study of molecular pathogenesis of radiation proctitis. *International journal of radiation oncology, biology, physics* 76, 242-250.
- Tian, Y., Ma, X., Lv, C., Sheng, X., Li, X., Zhang, R., Song, Y., Andl, T., Plikus, M.V., Sun, J., Ren, F., Shuai, J., Leighton, C.J., Cui, W., Yu, Z., 2017. Stress responsive miR-31 is a major modulator of mouse intestinal stem cells during regeneration and tumorigenesis. *Elife* 6.
- Vliegenthart, A.D.B., Berends, C., Potter, C.M.J., Kersaudy-Kerhoas, M., Dear, J.W., 2017. MicroRNA-122 can be measured in capillary blood which facilitates point-of-care testing for drug-induced liver injury. *Br J Clin Pharmacol* 83, 2027-2033.
- Wang, W.J., Wu, S.P., Liu, J.B., Shi, Y.S., Huang, X., Zhang, Q.B., Yao, K.T., 2013. MYC regulation of CHK1 and CHK2 promotes radioresistance in a stem cell-like population of nasopharyngeal carcinoma cells. *Cancer Res* 73, 1219-1231.
- Wang, Y., Liang, H., Jin, F., Yan, X., Xu, G., Hu, H., Liang, G., Zhan, S., Hu, X., Zhao,

- Q., Liu, Y., Jiang, Z.Y., Zhang, C.Y., Chen, X., Zen, K., 2019. Injured liver-released miRNA-122 elicits acute pulmonary inflammation via activating alveolar macrophage TLR7 signaling pathway. *Proceedings of the National Academy of Sciences of the United States of America* 116, 6162-6171.
- Yuan, Z., Ma, J., Meng, X., Chen, N., Shen, M., 2018. Chk2 deficiency alleviates irradiation-induced taste dysfunction by inhibiting p53-dependent apoptosis. *Oral Dis* 24, 856-863.
- Zheng, L., Han, X., Hu, Y., Zhao, X., Yin, L., Xu, L., Di, Y., Xu, Y., Han, X., Liu, K., Peng, J., 2019. Dioscin ameliorates intestinal ischemia/reperfusion injury via adjusting miR-351-5p/MAPK13-mediated inflammation and apoptosis. *Pharmacol Res* 139, 431-439.
- Zhou, Y., Ren, H., Dai, B., Li, J., Shang, L., Huang, J., Shi, X., 2018. Hepatocellular carcinoma-derived exosomal miRNA-21 contributes to tumor progression by converting hepatocyte stellate cells to cancer-associated fibroblasts. *J Exp Clin Cancer Res* 37, 224.

Table 1

Three patients' details.

| Patient | Gender | Age | TNM staging | IR Dose |
|---------|--------|-----|-------------|-----------|
| 1 | M | 60 | T4N2M0 III | 48 Gy/25F |
| 2 | F | 60 | T3N1M0 III | 52 Gy/25F |

| | | | | |
|---|---|----|------------|-----------|
| 3 | F | 59 | T4N2M0 III | 48 Gy/25F |
|---|---|----|------------|-----------|

M: Male; F: Female

Table 2

Primer sequences used in this study.

| miRNA/Gene | Primer sequence |
|----------------------|---|
| miR-122-5p | Forward 5'-GTGACAATGGTGGAATGTGG-3' Reverse 3'-CAGAACCGTAGCAAAACGAAA-5' |
| U6 | Forward 5'-CTCGCTTCAGCAGCACA-3' Reverse: 3'-TGCGTTTAAGCACTTCGCAA-5' |
| CCAR1 | Forward 5'-GTTC AACAGCCATCACTCCTTGGA-3' Reverse 3'-CTGTTGTTGCACACTATACAGGGC-5' |
| STK24 | Forward 5'-CTGGGCATAACAGCTATTGAAC-3' Reverse 3'-TGAGGGGTTTACTGTAGTTTCC-5' |
| OCLN | Forward 5'-AACTTCGCCTGTGGATGACTTCAG-3' Reverse 3'-GACTCGCCGCCAGTTGTGTAG-5' |
| GAPDH | Forward 5'-GAGTCAACGGATTTGGTCGT-3' Reverse 3'-TGGGATTTCATTGATGACA-5' |
| CCAR1 RNA(i)-1 | 5'-GGAGAATGGTGCCAGTGTA-3' |
| RNA(i)-2 | 5'-GAAGTAGAGTCCTTAGAAA-3' |
| miR-122-5p antagomir | 5'-CAAACACCAUUGUCACACUCCA-3' |
| NC | 5'-CAGUACUUUUGUGUAGUACAAA-3' |

| | |
|------------|------------------------------|
| miR-122-5p | 5'-UGGAGUGUGACAAUGGUGUUUG-3' |
| miR-NC | 5'-UUCUCCGAACGUGUCACGUTT-3' |

Figure Legends

Fig. 1. Irradiation upregulates miR-122-5p levels and promotes apoptosis *in vivo*.

(A) The miR-122-5p levels in the serum of rectal cancer patients before and after radiotherapy. (B) The miR-122-5p levels in mice rectal tissues at different time points (1 hour, 7 days, and 14 days) after IR or non-IR (n=5 mice/group). (C) Representative images of H&E, TUNEL, and cl-caspase-3-positive cells at above time point after IR or non-IR; magnification 200 \times . (D, E) Quantification of TUNEL and cl-caspase-3-positive cells at above time points after IR or non-IR. *p < 0.05, **p < 0.01, ***p < 0.001, ****p < 0.0001.

Fig. 2. MiR-122-5p enhances the radiosensitivity of HIEC cells.

(A) The transfection efficiency of miR-122-5p after 48 hours of transfection with miR-122-5p mimic. U6 was used as the endogenous control. (B) The radiosensitivity of HIEC cells transfected with miR-122-5p mimic exposed to various doses of IR. (C) The γ -H2AX foci formation of HIEC cells transfected with miR-122-5p mimic 48 hours after IR or non-IR. Scale bars: 5 μ m. (D) The number of γ -H2AX foci per cell was quantitated. (E) The alteration of mitochondrial membrane potential ($\Delta\Psi$ m) in HIEC cells transfected with miR-122-5p mimic 48 hours after IR or non-IR. Scale bar: 50

μm . (F) The apoptosis of HIEC cells transfected with miR-122-5p mimic 48 hours after IR or non-IR. (G) The percentage of apoptotic cells was quantified. * $p < 0.05$, ** $p < 0.01$, *** $p < 0.001$, **** $p < 0.0001$, ns: no significance.

Fig. 3. CCAR1 is a direct target of miR-122-5p. (A, B) The Venn diagram of the potential targets of miR-122-5p. (C) The mRNA levels of three selected targets (CCAR1, OCLN, and STK24) in HIEC cells transfected with miR-122-5p mimic. (D) The specific locations of miR-122-5p binding sites in CCAR1 3'-UTR and mutant complementary sequences of the 3'-UTR of CCAR1 mRNA. (E) Luciferase activity was measured 48 hours later and renilla luciferase activity was used for normalization. (F) The protein levels of CCAR1 in HIEC cells transfected with miR-122-5p mimic. ** $p < 0.01$, **** $p < 0.0001$, ns: no significance.

Fig. 4. Silencing CCAR1 enhances DNA damage in HIEC cells. (A, B) The mRNA and protein levels of CCAR1 in HIEC cells after 48 hours of transfection with CCAR1 siRNA. GAPDH was used as the endogenous control. (C, D) The radiosensitivity of HIEC cells transfected with CCAR1 siRNA exposed to various doses of IR. (E, F) The γ -H2AX foci formation of HIEC cells transfected with CCAR1 siRNA 48 hours after IR or non-IR. (G, H) The number of γ -H2AX foci per cell was quantitated. Scale bar: 5 μm . * $p < 0.05$, ** $p < 0.01$, **** $p < 0.0001$, ns: no significance.

Fig. 5. Silencing CCAR1 promotes the apoptosis of HIEC cells. (A, B) The alteration of mitochondrial membrane potential ($\Delta\Psi_m$) in HIEC cells transfected with CCAR1 siRNA 48 hours after IR or non-IR. Scale bar: 50 μm . (C, D) The apoptosis of HIEC cells transfected with CCAR1 siRNA 48 hours after IR or non-IR. (E, F) The percentage of apoptotic cells was quantified. ** $p < 0.01$, *** $p < 0.001$.

Fig. 6. miR-122-5p downregulates p-CHK2 levels through CCAR1 in HIEC cells after IR treatment. (A, B) The protein levels of CHK2 and p-CHK2 in HIEC cells transfected with miR-122-5p mimic or CCAR1 siRNA 48 hours after IR or non-IR. (C) The protein levels of CHK2 and p-CHK2 in HIEC cells transfected with miR-122-5p mimic, CCAR1 siRNA, or miR-122-5p mimic+pcDNA3.1-CCAR1 48 hours after IR or non-IR. Actin was used as the endogenous control.

Fig. 7. MiR-122-5p inhibition alleviates radiation-induced rectal injury *in vivo*. (A) Schematic diagram of mice IR and miR-122-5p antagomir treatment. (B) The miR-122-5p levels in mice rectal tissues after IR combined treatment with miR-122-5p antagomir (n=5 mice/group). (C) Representative images of H&E, TUNEL, cI-caspase-3, CCAR1, and p-CHK2-positive cells in rectal tissues after IR combined treatment with miR-122-5p antagomir; magnification 200 \times . (D, E, F, and G) The quantification of TUNEL, cI-caspase-3, CCAR1, and p-CHK2-positive cells. ** $p < 0.01$, *** $p < 0.001$, **** $p < 0.0001$.

Fig 8. Schematic diagram of the molecular mechanism of miR-122-5p on radiation-induced rectal injury.

Journal Pre-proof

Author contributions:

LY and WYM were mainly responsible for the project design and guidance. GYL and TWZ worked together on most of the experiments. LJJ, CXM and CY completed data statistics analysis. XY and XYQ proofread the data. GYL wrote the manuscript. LY and TWZ made the revision.

Journal Pre-proof

Declaration of interests

The authors declare that they have no known competing financial interests or personal relationships that could have appeared to influence the work reported in this paper.

The authors declare the following financial interests/personal relationships which may be considered as potential competing interests:

Journal Pre-proof

1. MiR-122-5p levels were correlated with rectal injury severity induced by radiotherapy.
2. MiR-122-5p enhanced the radiosensitivity of human intestinal epithelial crypt (HIEC) cells.
3. MiR-122-5p aggravated radiation-induced rectal injury by targeting CCAR1, which maybe relate with CHK2.